Talanta 99 (2012) 69–74

Contents lists available at SciVerse ScienceDirect

Talanta

journal homepage: www.elsevier.com/locate/talanta

Highly sensitive synchronous fluorescence determination of mercury (II) based on the denatured ovalbumin coated CdTe QDs ☆

Yan-Qin Wang [a], Yang Liu [a], Xi-Wen He [a], Wen-You Li [a,*], Yu-Kui Zhang [a,b]

[a] State Key Laboratory of Medicinal Chemical Biology, and Department of Chemistry, Nankai University, Tianjin 300071, China
[b] National Chromatographic Research and Analysis Center, Dalian Institute of Chemical Physics, Chinese Academy of Sciences, Dalian 116011, China

ARTICLE INFO

Article history:
Received 10 January 2012
Received in revised form
19 April 2012
Accepted 30 April 2012
Available online 22 May 2012

Keywords:
Denatured ovalbumin coated CdTe QDs
Synchronous fluorescence
Mercury (II) determination
Probe

ABSTRACT

Chemically denatured ovalbumin (dOB) was used to modify the surface of 3-mercaptopropionic acid (MPA) stabilized CdTe quantum dots (QDs), which resulted in a great enhancement of the synchronous fluorescence intensity. Moreover, dOB shell layer can effectively prevent the binding of other cations onto the QDs core and enhance the selective binding ability of Hg^{2+} to dOB coated CdTe QDs (CdTe-dOB QDs). A simple method with high sensitivity and selectivity was developed for the determination of Hg^{2+} with the CdTe-dOB QDs as fluorescence probe based on the merits of synchronous fluorescence spectroscopy (SFS). When scanning with excitation and emission wavelengths of 250 nm and 470 nm ($\Delta\lambda=\lambda_{em}-\lambda_{ex}=220$ nm), respectively, the maximum synchronous fluorescence peak of the CdTe-dOB QDs was located at 328 nm. Under optimal conditions, the change of the synchronous fluorescence intensity was in good linear relationship with the Hg^{2+} concentration in the range of 0.08×10^{-7} to 30.0×10^{-7} mol L^{-1} and the detection limit was 4.2×10^{-9} mol L^{-1} ($S/N=3$). The relative standard deviation of seven replicate measurements for the concentration of 2.0×10^{-7} mol L^{-1} and 20.0×10^{-7} mol L^{-1} were 2.8% and 2.3%, respectively. Compared with general fluorescence methods, the proposed method, which combined the advantages of high sensitivity of synchronous fluorescence and specific response of Hg^{2+} to CdTe-dOB, had a wider linear range and higher sensitivity. Furthermore, the proposed method was applied to the determination of trace Hg^{2+} in water samples with satisfactory results.

1. Introduction

Heavy metal mercury is a hazardous contaminant of environment which can be accumulated in organisms and interact with the proteins and thymine–thymine bases in DNA duplexes [1] to cause a serious threat to human health even at very low concentration level [2,3]. The development of new methods for the quantification of mercury at ultra-trace levels is a challenging task and one of considerable interests. Traditional methods such as atomic absorption spectrometry (AAS) and inductively coupled plasma mass spectrometry (ICP-MS) to detect mercury ions are often costly, time-consuming and not appropriate for point-of-use applications [4], so there is a strong demand to develop a novel method with the advantages of the few interference, facile fabrication process, and low cost. The advantages of fluorescence signaling in its intrinsic sensitivity have encouraged the development of a variety of fluorescent sensors for the detection of metal ions [5–7]. As new type of fluorescent sensors, QDs offer a number of attractive features, including high photobleaching threshold, good chemical stability, relatively broad and symmetric luminescence bands [8,9], which wished to remedy the deficiencies of the fluorescent dyes. In order to improve the chemical stability and bio-compatibility, and reduce the toxicity of the QDs, biomolecules were usually selected as coating layer for QDs. Up to now, biomolecules are linked to QDs mainly by covalent attachment [10–13], electrostatic attraction [14–16], etc. For example, with the help of 1-ethyl-3-(3-(dimethylamine)propyl) carbodiimide hydrochloride (EDC) and N-hydroxysuccinimide (NHS), bovine serum albumin (BSA) was conjugated to TGA-capped CdTe QDs via an amide link interacting with carboxyl of the TGA-capped CdTe, which could develop a novel fluorescent nanosensor for Sb^{3+} determination [17]. Wang et al. [18] and Kuo et al. [19] used $NaBH_4$ as reducing agents to promote the disulfide bonds in the BSA molecule being converted to sulfhydryl groups. The thiol group of denatured BSA has strong affinity to Cd atom, so the dBSA was modified to the QDs surface [18], which demonstrated a great enhancement of the fluorescence intensity and stability. Compared with the amide linking method, Huang's research was

☆ Novelty statement: This paper aimed at combining the advantages of the high sensitivity of synchronous fluorescence technique in analysis, with the specific selectivity of Hg^{2+} to the denatured OB coated CdTe QDs, to develop a novel fluorescence probe for the determination of Hg^{2+} in water samples.

* Corresponding author. Tel.: +86 22 23494962; fax: +86 22 23502458.
E-mail address: wyli@nankai.edu.cn (W.-Y. Li).

0039-9140/$ - see front matter © 2012 Elsevier B.V. All rights reserved.
http://dx.doi.org/10.1016/j.talanta.2012.04.064

not only easy to operate, but also provided a new approach for the conjugation of QDs and proteins. Chemically denatured ovalbumin (dOB) had also been conjugated to the surface of CdTe QDs [20,21], which has efficiently improved the chemical stability and fluorescence intensity of the QDs and developed as temperature insensitive bioprobes [20] or protein probes [21]. Later on, it was demonstrated by Xia and Zhu [22] that the fluorescence of dBSA-coated CdTe QDs could be quenched by Hg^{2+} with high sensitivity and selectivity, while other cations could hardly quench the fluorescence even at fairly higher concentration levels because the denatured protein shell layer effectively prevented the binding of cations onto the QD core [22]. Based on these facts, the denatured protein shell protected QDs could be developed as highly selective probe for Hg^{2+} determination. Though previously developed methods had satisfactory low detection limit, when coming to the complicated component realistic samples which contain multiple fluorescent species, the general fluorescence method could not avoid the spectra interference and simplify the emission spectra. Compared with general fluorescence, the synchronous fluorescence spectra (SFS) was a multidimensional fluorescence technique which involves in scanning simultaneously by the excitation and emission monochromators while maintaining a constant wavelength interval ($\Delta\lambda$) between λ_{ex} and λ_{em} [23]. This technique could not only maintain the sensitivity, but also simplify the emission spectra, improve the selectivity and spectral resolution, decrease the interference due to light scattering [24,25]. So this paper aimed at combining the advantages of the high sensitivity of synchronous fluorescence technique in analysis with the specific selectivity of Hg^{2+} to the denatured OB coated CdTe QDs, to develop a novel fluorescence probe for the determination of Hg^{2+} in water samples.

2. Experimental

2.1. Apparatus and reagents

UV–vis absorption spectra were recorded at room temperature with a UV-2450 UV–vis spectrophotometer (Shimadzu, Japan). The synchronous fluorescence spectra were performed using a F-4500 fluorescence spectrophotometer (Hitachi, Japan). The high-resolution transmission electron microscopy (HRTEM) image of the nanoparticles was acquired on a Tecnai G2 F20 transmission electron microscope with the voltage of 200 KV (Philips, Holland). Fourier transform infrared (FTIR) spectra were recorded on a Magna-560 spectrometer (Nicolet, USA). AF-610D cold vapor-atomic fluorescence spectrometry (CV-AFS) (Beijing Rayleigh Analysis Instrument Company, China) was used for the determination of Hg^{2+} in water samples. All pH values were measured with a pHSJ-3F digital pH meter (Analytical Instruments Co., Tianda, China).

Tellurium power (99%), $CdCl_2 \cdot 2.5H_2O$ and $NaBH_4$ (99%) were purchased from J & K Chemical Co. 3-Mercaptopropionic acid (MPA, 99%) and Glycine (99%) were purchased from Alfa Aesar. Ovalbumin (OB, 98%) and Tris(hydroxymethyl) aminomethane (Tris, 99.8%) were from Sigma. Hg $(NO_3)_2$ standard samples was acquired from YuDa chemical reagent Co. Ltd. (Tianjin, China). Britton–Robinson (B–R) buffer solution were prepared by mixing 0.04 mol L^{-1} H_3PO_4–CH_3COOH–H_3BO_3 solution and 0.2 mol L^{-1} of NaOH solution to the required pH value. All the chemicals used were of analytical-reagent grade and all the solutions were prepared with double deionized water (DDW).

2.2. Procedures

2.2.1. Preparation of CdTe QDs

The preparation of 3-mercaptopropionic acid (MPA)-capped CdTe QDs was performed according to previous reports with some modification [26,27]. In brief, freshly prepared oxygen-free NaHTe solution was added to nitrogen-saturated $CdCl_2$ aqueous solution (pH 9) in the presence of MPA as a stabilizing agent. The ratio of $CdCl_2$:MPA:NaHTe was fixed at 2:4.8:1. The resulting mixture was then subjected to refluxing to control the size of the CdTe QDs.

2.2.2. Preparation of denatured ovalbumin coated CdTe QDs

Denatured ovalbumin was prepared by chemically treating ovalbumin with $NaBH_4$ [19] as following steps: 0.11 g ovalbumin was dissolved in 50 mL of deionized water, then 0.004 g of $NaBH_4$ was added under stirring. The reaction proceeded at room temperature for 1 h and then at 70 °C for 30 min until no more gas (H_2) was generated. The final concentration of dOB aqueous solution was 5.0×10^{-5} mol L^{-1}. The MPA coated CdTe QDs were precipitated with ethanol and then isolated by centrifugation and decantation to remove free MPA molecules. Then it was redissolved into a certain amount of denatured ovalbumin solution [21,22]. The resulting solution was incubated at 70 °C under stirring for 30 min.

2.2.3. Procedure for the synchronous fluorescence detection of Hg^{2+}

In a series of 10 mL calibrated test tubes, 2.5 mL of as-prepared CdTe-dOB ($C_{dOB}/C_{QDs}=1/10$) solution (2.0×10^{-4} mol L^{-1}), 1.0 mL of B–R buffer solution (pH 9.0), and various amounts of Hg^{2+} were added, then the mixture was diluted to the mark with DDW and mixed thoroughly for measurements after 20 min. When scanning with excitation wavelengths of 250 nm and emission wavelength of 470 nm ($\Delta\lambda=\lambda_{em}-\lambda_{ex}=220$ nm), the synchronous fluorescence intensities of the CdTe-dOB QDs in the absence (I_{SF0}) and presence (I_{SF}) of Hg^{2+} were measured at $\lambda=328$ nm. The slit widths of excitation and emission were 5 nm and 10 nm, and PMT voltage, 700 V.

3. Results and discussion

3.1. TEM characterization of CdTe-dOB QDs

After ovalbumin was denatured and most of its disulfide bonds were converted to sulfhydryl groups, it formed a linear structure multi-thiol-group denatured OB (dOB). When CdTe QDs were incubated in the dOB solution, the dOB could coat the surface of QDs through ligand exchange and a complex of $CdTe_x(dOB)_{1-x}$ could be formed as shown in Scheme 1. The morphology of the as-prepared CdTe-dOB QDs was studied by HRTEM (Fig. 1). It could be seen that the nanoparticles still showed obvious crystal lattices. The modification of the QDs surfaces with dOB molecule did not result in any aggregation. The CdTe-dOB QDs were spherical and monodisperse with a particle size of about 2.6 ± 0.3 nm which was nearly the same size as the original CdTe QDs. The reason may be that the light atoms or proteins in the shell did not contribute to the signal in the TEM images. The same phenomenon can also be seen in the TEM image of protein BSA-stabilized Au_{25} nanoclusters, in which only the Au core could be seen, while the BSA shell could not be seen in the TEM image [28].

3.2. UV–vis and synchronous fluorescence feature of CdTe QDs and CdTe-dOB QDs

The optical properties of original CdTe QDs and CdTe-dOB QDs were characterized by the UV–visible absorption spectrophotometry and synchronous fluorescence spectrophotometry. After modification of the QDs surface with denatured ovalbumin, the results showed a blue shift of the first excitonic absorbance peaks from 518.8 nm in Fig. 2A, curve (a), to 514 nm, curve (b). The particle size of the prepared CdTe-dOB QDs was calculated to be

2.68 nm from the first excitonic absorption peak of UV spectra by using Peng's method [29]. The synchronous fluorescence spectra obtained from CdTe QDs and CdTe-dOB QDs were also shown in Fig. 2B. As can be seen in Fig. 2B, a blue shift of the synchronous fluorescence peak of wavelengths from 340 nm in Fig. 2B, curve (a), to 328 nm, curve (b), appeared which meant the size of the inner CdTe "core" had a little decrease. The reason may be that when denatured ovalbumin was conjugated onto the CdTe surface, some Te atoms were dissociated from the surface of QDs, which resulted in the core size decrease, so the first excitonic absorbance peak and maximum synchronous fluorescence peak showed the blue shift. The conjugation of denatured ovalbumin onto the CdTe surface formed the $CdTe_x$(denatured ovalbumin)$_{1-x}$ complex [21,22], which resulted in the great enhancement of the synchronous fluorescence intensity.

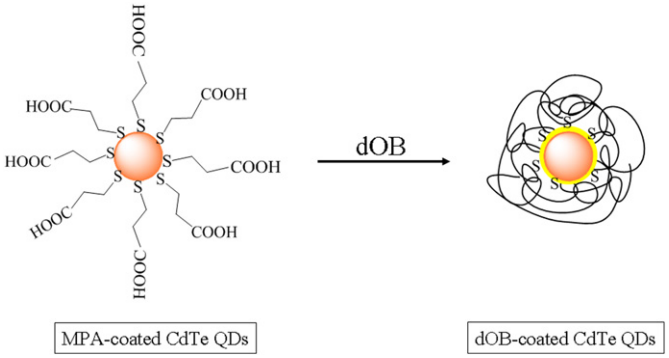

Scheme 1. Schematic representation of the modification of CdTe QDs by the denatured ovalbumin.

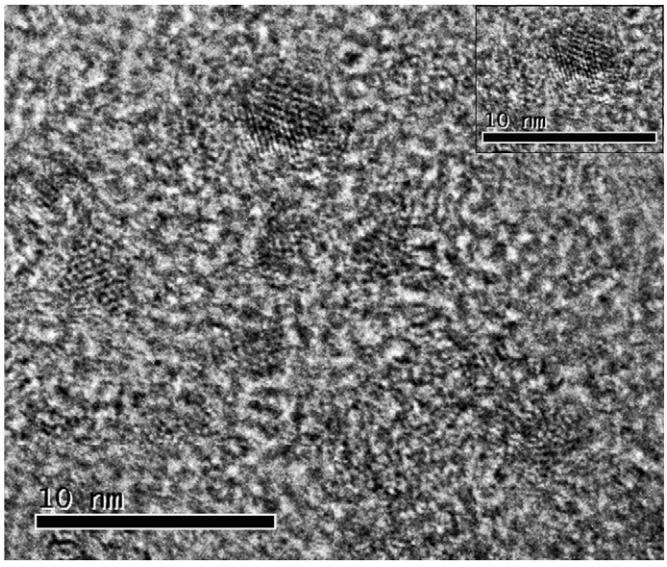

Fig. 1. HRTEM image of denatured OB coated CdTe QDs (CdTe-dOB QDs).

3.3. Fourier transform infrared spectrum

Fourier transform infrared (FTIR) spectra were used to prove the substitution of MPA with dOB on CdTe QDs surfaces (Fig. 3). For QDs-MPA, asymmetric and symmetric stretching bands of –COO– located at 1560 and 1400 cm^{-1}, respectively, were the most distinctive bands. The C–O stretch vibrational of MPA-QDs at 1030 cm^{-1} and C–S at 667 cm^{-1} were also observed in the IR spectrum (curve (a)). The primary bands of interest for dOB included the amide I band at 1650 cm^{-1} and the amide II band

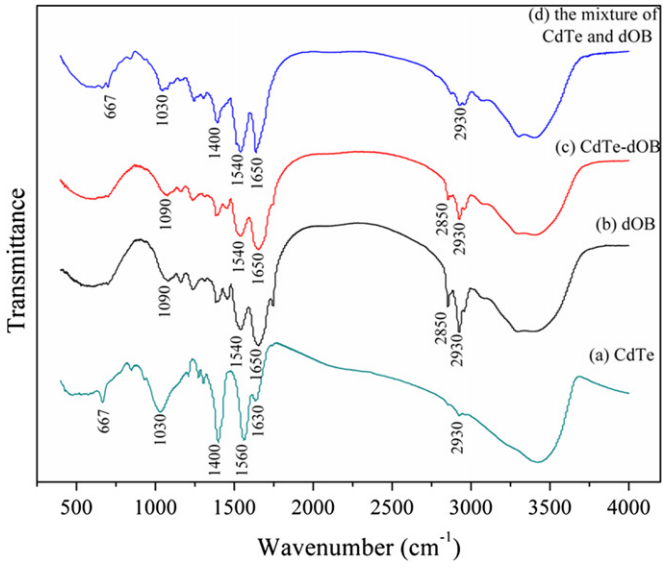

Fig. 3. Fourier Transform Infrared (FTIR) spectra of 3-mercaptopropionic acid (MPA)-capped CdTe QDs (a), denatured ovalbumin (dOB) (b), denatured ovalbumin (dOB)-coated CdTe QDs (c) and mixture of dOB and 3-mercaptopropionic acid (MPA)-capped QDs (d).

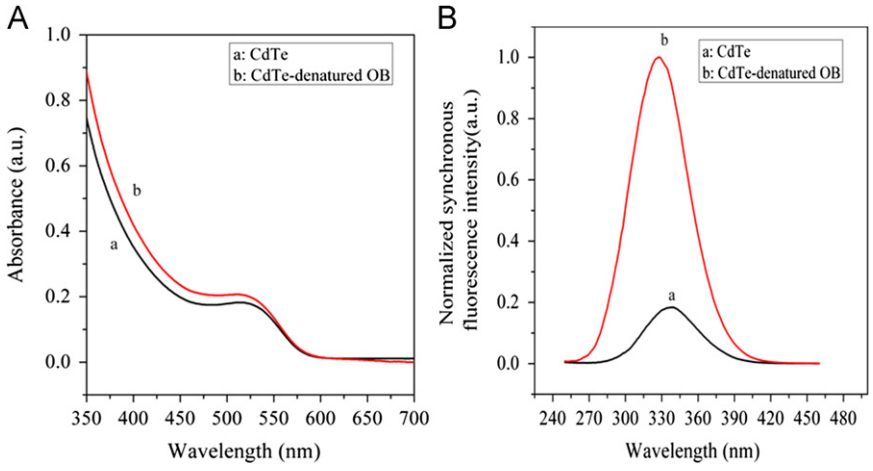

Fig. 2. UV–vis absorption spectra (A) and synchronous fluorescence spectra (B) of CdTe QDs and CdTe-dOB QDs (dOB:CdTe=1:10) with the same concentration (2.0×10^{-4} mol L^{-1}).

at 1540 cm^{-1} (curve (b)) [19]. When dOB and MPA-coated CdTe QDs were simply mixed, IR spectra showed the peaks from the overlap result of two separate samples, as shown in the curve (d). However, when the dOB-coated CdTe QDs was formed, only the IR spectrum (curve (c)) identical to that of dOB (curve (b)) was observed, suggesting that the MPA molecules on the CdTe QD surfaces have almost completely been replaced by dOB molecules.

3.4. Optimal ratio of denatured ovalbumin to QDs

To choose the optimal modification ratio of denatured ovalbumin to QDs, we prepared a series of aqueous solutions with the same QDs concentration (2.5×10^{-5} mol L^{-1}) but different ratios of dOB to QDs, and investigated the changes of synchronous fluorescence peak positions and intensities as functions of dOB concentration (Fig. 4). As shown in Fig. 4, with the increasing ratio of denatured ovalbumin to QDs, the synchronous fluorescence peak showed continuous blue shift for as much as 15 nm. Moreover, synchronous fluorescence intensity of the CdTe-dOB increased gradually at first and then began to decrease when the concentration of denatured ovalbumin is higher than 2.5×10^{-6} mol L^{-1}, which meant that when conjugating the QDs with denatured ovalbumin, excess denatured ovalbumin do not contribute to the enhancement of the synchronous fluorescence intensity. It was speculated that the passivation of QDs surface with denatured ovalbumin led to the increase of the synchronous fluorescence intensity. On the basis of the above-mentioned experimental results, the optimal molar ratio of denatured ovalbumin to QDs was chosen as 1:10.

3.5. Synchronous fluorescence characteristics of the CdTe-dOB-Hg^{2+} system

The effect of Hg^{2+} on the synchronous fluorescence emission of the CdTe-dOB QDs was shown in Fig. 5. When $\Delta\lambda = 220$ nm (scanning with excitation and emission wavelengths of 250 and 470 nm, respectively), the synchronous fluorescence peak of CdTe-dOB QDs was located at 328 nm. Furthermore, the maximum fluorescence intensity of CdTe-dOB QDs was significantly quenched with the increasing of Hg^{2+} concentration in the range of $0.08–30 \times 10^{-7}$ mol L^{-1}. The quenching effect of Hg^{2+} on the synchronous fluorescence emission of CdTe-dOB QDs was found to be concentration dependent. The phenomena indicated that the SFS could be used for the development of a sensitive and selective method for the determination of Hg^{2+}.

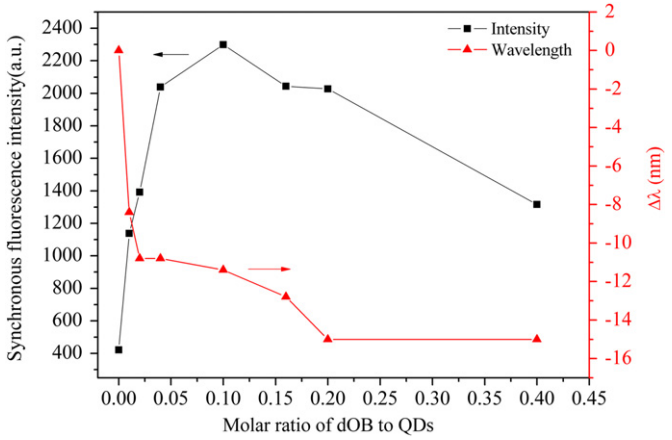

Fig. 4. The synchronous fluorescence intensity and wavelength shift of a series of CdTe-dOB solutions with the same CdTe QDs concentration (2.5×10^{-5} mol L^{-1}) but different molar ratio of dOB to QDs.

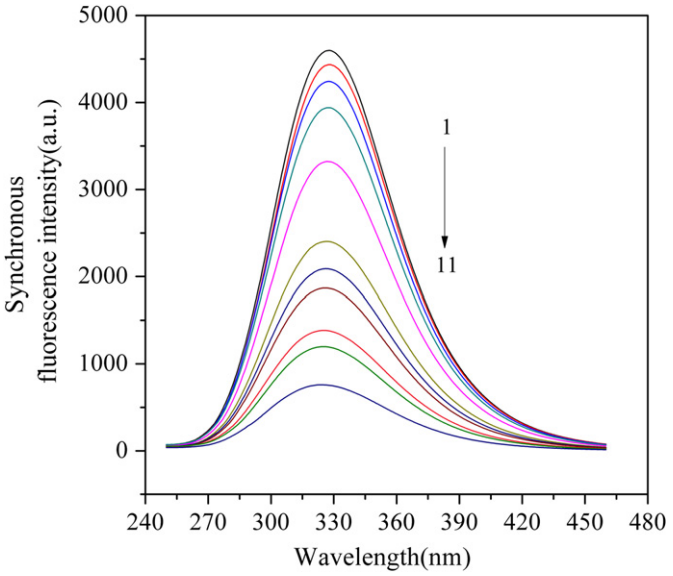

Fig. 5. Effect of the concentration of Hg^{2+} on synchronous fluorescence intensity of the CdTe-dOB QDs. CdTe-dOB: 5.0×10^{-5} mol L^{-1}, B–R buffer (1.0 mL, pH=9.0); from 1 to 11, the concentration of Hg^{2+} were 0, 0.08, 0.5, 0.8, 2, 5, 8, 10, 15, 20 and 30×10^{-7} mol L^{-1}, respectively.

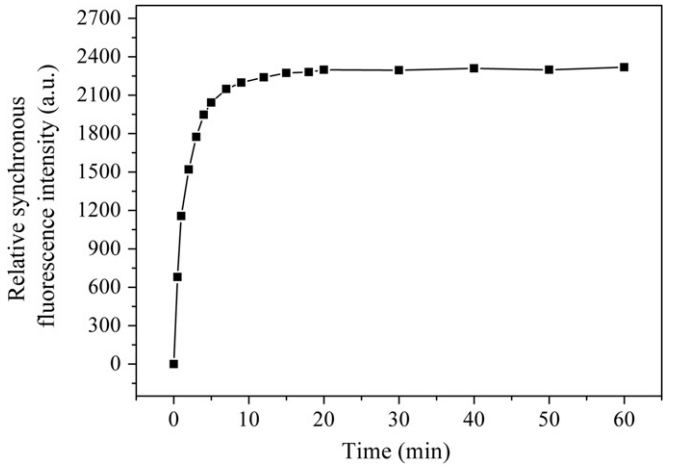

Fig. 6. Effect of time on the relative synchronous fluorescence intensity. CdTe-dOB, 5.0×10^{-5} mol L^{-1}; Hg^{2+} and 5.0×10^{-7} mol L^{-1}; B–R buffer (1.0 mL, pH=9.0).

3.6. Factors affecting the fluorescence detection for Hg^{2+} with CdTe-dOB QDs

In order to optimize the conditions for the detection of Hg^{2+} with the CdTe-dOB QDs, synchronous fluorescence intensity of the CdTe-dOB QDs solution in the absence of Hg^{2+} (I_{SF0}) and presence of Hg^{2+} (I_{SF}) were determined, respectively. Then, the effects of reaction time, pH and the concentration of CdTe-dOB QDs on the relative synchronous fluorescence intensity ($\Delta I_{SF} = I_{SF0} - I_{SF}$) of the CdTe-dOB QDs solution were investigated as follows.

3.6.1. Reaction time and mixing sequence

According to the experimental results (Fig. 6), the reaction between CdTe-dOB QDs and Hg^{2+} reached the equilibrium within 20 min, and the relative synchronous fluorescence signals were stable for at least 60 min at room temperature. In addition, after investigating the mixing sequences, it was found that the best order was to mix CdTe-dOB QDs and B–R buffer solution first, and

then Hg^{2+}. Therefore, all the measurements were made after CdTe-dOB QDs, B–R buffer solution and Hg^{2+} were completely mixed for 20 min.

3.6.2. Effect of pH

The influence of different kinds of buffers on the relative synchronous fluorescence intensity of the system was studied by using Britton–Robinson (B–R) buffer, Tris–HCl and glycine–NaOH buffers at pH values in a range from 8.0 to 10.5, as shown in Fig. 7. It can be found that with the increasing of pH values, the maximum relative synchronous fluorescence intensity occurred at pH 9.0 when using Britton–Robinson buffer. In addition, when varying the volume of the buffer from 0.5 mL to 2.5 mL, relative synchronous fluorescence intensities changed slightly, so 1.0 mL of B–R buffer (pH 9.0) solution was adopted.

3.6.3. Effect of the concentration of CdTe-dOB

The effect of the CdTe-dOB QDs concentration on the relative synchronous fluorescence intensity was also investigated (Fig. 8). At first, with the increasing concentration of CdTe-dOB QDs, the synchronous fluorescence intensity difference of the system increased significantly. After the concentration of CdTe-dOB QDs reached 4.0×10^{-5} mol L^{-1}, the relative fluorescence intensity changed slightly. When the concentration of CdTe-dOB QDs was higher than 5.0×10^{-5} mol L^{-1}, the relative fluorescence intensity began to drop down. So the concentration of CdTe-dOB QDs was selected as 5.0×10^{-5} mol L^{-1} for further research.

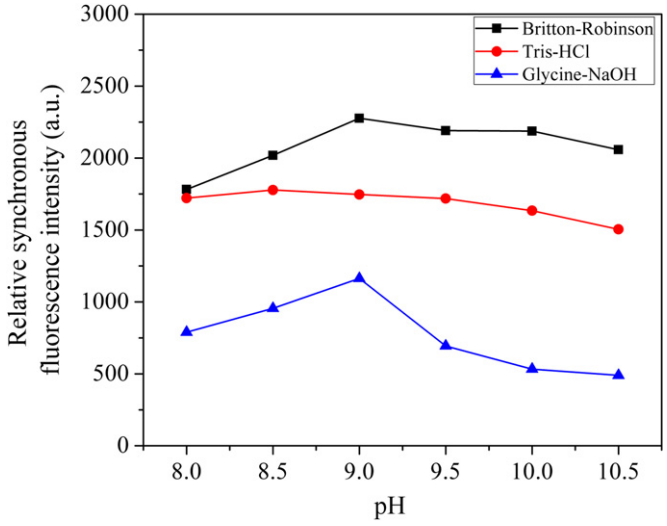

Fig. 7. Effects of the buffer pH on the relative synchronous fluorescence intensity. (■) Britton–Robinson; (●) Tris–HCl; (▲) Glycine–NaOH. CdTe-dOB, 5.0×10^{-5} mol L^{-1}; Hg^{2+}, 5.0×10^{-7} mol L^{-1}; buffer volume (1.0 mL).

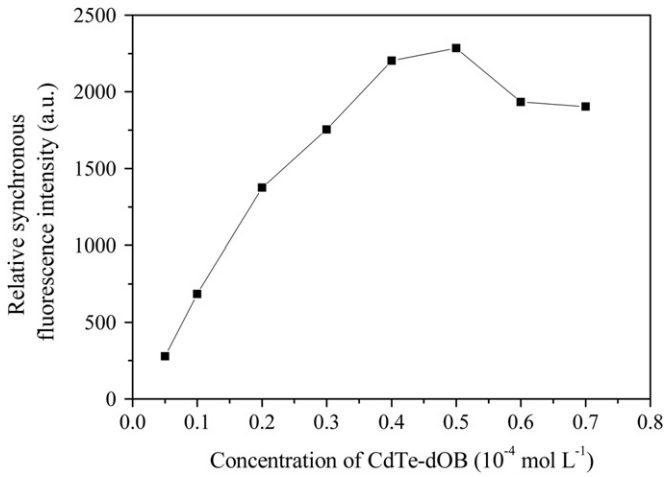

Fig. 8. Effect of the concentration of CdTe-dOB QDs on the relative synchronous fluorescence intensity. Hg^{2+}, 5.0×10^{-7} mol L^{-1}; B–R buffer (1.0 mL, pH=9.0).

3.6.4. Effect of potential interfering ions

The influence of various coexistence ions on the synchronous fluorescence of CdTe-dOB QDs-Hg^{2+} system was tested to evaluate the selectivity of the proposed method (Table 1). The experiments were carried out by fixing the concentration of Hg^{2+} at 0.5 μmol L^{-1} and then recording the change of synchronous fluorescence intensity before and after adding the potential interfering ions into the solution. With a tolerance level of ±5%, it can be found that some ions show little interference and could exist in at least 2000-fold more than the concentration of Hg^{2+}. In the experiments, Cu^{2+} showed the major interference, so a proper amount of thiourea solutions can be added as masking agents [30]. The mercury (I) was also a major interference when it was co-existed with the mercury (II) in the determination system. However, this species of mercury rarely existed in the real water samples. Consequently, this method is suitable for the analysis of Hg^{2+} in water samples.

3.7. Analytical performance of CdTe-dOB QDs for Hg^{2+}

Under the optimal conditions, it was found that Hg^{2+} quenched the synchronous fluorescence intensity of CdTe-dOB in a concentration dependence that is best described by a Stern–Volmer equation:

$$I_{SF0}/I_{SF} = K_{sv}[Q]+1$$

I_{SF0} and I_{SF} are the synchronous fluorescence intensity of the CdTe-dOB in the absence and presence of Hg^{2+} ion, respectively. K_{sv} is the Stern–Volmer quenching constant and [Q] is the concentration of Hg^{2+}. The calibration plot of I_{SF0}/I_{SF} versus Hg^{2+} concentration [Q] showed a good linear relationship (R=0.995) in the range from 0.08×10^{-7} to 30.0×10^{-7} mol L^{-1}. K_{sv} was found to be 1.58×10^{6} L mol^{-1}. The limit of detection (LOD), calculated by the equation LOD=$3S_b/K_{sv}$, where S_b was the standard deviation of blank measurements (n=8) and K_{sv} was the slope of calibration graph, 4.2×10^{-9} mol L^{-1}. The relative standard deviations of seven replicate measurements for 2.0×10^{-7} mol L^{-1} and 20.0×10^{-7} mol L^{-1} were 2.8% and 2.3%,

Table 1
Interference of different metal ions on the synchronous fluorescence intensity of CdTe-dOB-Hg^{2+} system.

Coexisting metal ions[a]	Concentration (μmol L^{-1})	Variation of the calculated value (%)
K^+	1000	−2.8%
Na^+	1000	−4.8%
Ca^{2+}	100	+1.0%
Mg^{2+}	100	+0.2%
Fe^{3+}	1	−2.6%
Co^{2+}	1	−1.1%
Ni^{2+}	2	−1.3%
Mn^{2+}	1	−1.8%
Zn^{2+}	10	−0.3%
Pb^{2+}	1	−2.7%
Ba^{2+}	10	−4.8%
Cu^{2+}	0.1	−2.6%
Bi^{3+}	10	+1.3%
Hg_2^{2+}	0.1	−4.0%

[a] Concentration of Hg^{2+} is 0.5 μmol L^{-1}, CdTe-dOB, 5.0×10^{-5} mol L^{-1}; B–R buffer (1.0 mL, pH=9.0).

Table 2
Comparison of the main characteristics of QDs-based sensing systems for the determination of Hg^{2+}.

Probe [a]	Linear range (mol L^{-1})	LOD (mol L^{-1})	References
MAA-CdS QDs	$0.05–4.0\times10^{-7}$	4.2×10^{-9}	[2]
QDs at SiO_2-Rh6G	$0.4–8.0\times10^{-7}$	2.59×10^{-9}	[7]
dBSA-CdTe QDs	$0.12–15.0\times10^{-7}$	4.0×10^{-9}	[22]
GSH-CdS QDs	$0.15–125.0\times10^{-7}$	4.5×10^{-9}	[31]
Bi-color CdTe QDs multilayer films	$0.1–10\times10^{-7}$	4.5×10^{-9}	[32]
NAC-capped ZnS QDs	$0–2.4\times10^{-6}$	5.0×10^{-9}	[33]
Quantum dots-multilayer film	$0.05–5.0\times10^{-7}$	–	[34]
This work	$0.08–30.0\times10^{-7}$	4.2×10^{-9}	–

[a] Abbreviations of the reagents: MAA, Mercaptoacetic acid; Rh 6G, Rhodamine 6G; dBSA, denatured bovine serum albumin; GSH, glutathione; NAC, N-acetyl-l-cysteine.

Table 3
Determination of Hg^{2+} in water samples with the CdTe-dOB based SFS method.

Sample	Added (10^{-7} mol L^{-1})	Found (10^{-7} mol L^{-1})[a]	Foundby CV-AFS (10^{-7} mol L^{-1})	Recovery (%)
Tap water	0.50	0.51 ± 0.04	0.51	102.6
	2.00	1.99 ± 0.03	1.98	99.7
	0.50	0.50 ± 0.03	0.49	99.6
Lake water[b]	2.00	2.03 ± 0.04	1.97	101.3

[a] Mean of five experiments ± standard deviation.
[b] Lake water at Nankai University, Tianjin.

respectively. The main characteristics for fluorimetric determination of Hg^{2+} with QDs systems [2,7,22,31–34] were summarized in Table 2

The proposed method has been applied to the determination of Hg^{2+} in water samples (Table 3). The water samples were filtered four times through qualitative filter paper before use. The real samples (tap water and lake water) analysis results showed that Hg^{2+} could not be detected directly in them, and the results were obtained by applying the standard addition method. The accuracy of this method was evaluated by determining the recoveries of Hg^{2+} in the water samples by standard addition method. From Table 3, it can be seen that the recoveries for four samples were found to be in the range of 99.6%–102.6% and the determination results of the proposed method were in agreement with the results obtained by cold vapor-atomic fluorescence spectrometry (CV-AFS), which suggested that the method is reliable and practical.

4. Conclusion

In summary, denatured ovalbumin was used as capping agents to modify the surface of water-soluble CdTe QDs. The CdTe-dOB QDs has been developed as a sensitive and selective fluorescence probe for Hg^{2+} determination based on the synchronous fluorescence technique. Compared with the general fluorescence method, this SFS method showed high sensitivity and wide linear range. Based on the strong quenching effect of Hg^{2+}, a very good linear relationship was observed in Hg^{2+} concentration ranging from 0.08×10^{-7} to 30.0×10^{-7} mol L^{-1} with a low detection limit (4.2×10^{-9} mol L^{-1}). Furthermore, it also demonstrated the feasibility of the synchronous fluorescence spectroscopy as a promising Hg^{2+} determination approach in water samples.

Acknowledgments

This work was supported by the National Basic Research Program of China (973 Program) (Nos. 2011CB707703 and 2012CB910601), the National Natural Science Foundation of China (no. 21075069), and the Tianjin Natural Science Foundation (No. 11JCZDJC21700).

References

[1] Y.H. Lin, W.L. Tseng, Anal. Chem. 82 (2010) 9194–9200.
[2] M. Koneswaran, R. Narayanaswamy, Sens. Actuators B: Chem. 139 (2009) 91–96.
[3] B.K Jena, C.R. Raj, Anal. Chem. 80 (2008) 4836–4844.
[4] K. Leopold, M. Foulkes, P. Worsfold, Anal. Chim. Acta 663 (2010) 127–138.
[5] M. Koneswaran, R. Narayanaswamy, Sens. Actuators B: Chem. 139 (2009) 104–109.
[6] H.Q. Chen, A.N. Liang, L. Wang, Y. Liu, B.B. Qian, Microchim. Acta 164 (2009) 453–458.
[7] H.Z. Liu, P. Yu, D. Du, C.Y. He, B. Qiu, X. Chen, G.N. Chen, Talanta 81 (2010) 433–437.
[8] I.L. Medintz, H.T. Uyeda, E.R. Goldman, H. Mattoussi, Nat. Mater. 4 (2005) 435–446.
[9] W.C.W. Chan, D.J. Maxwell, X.H. Gao, R.E. Bailey, M.Y. Han, S.M. Nie, Curr. Opin. Biotechnol. 13 (2002) 40–46.
[10] M. Bruchez Jr, M. Moronne, P. Gin, S. Weiss, A.P. Alivisatos, Science 281 (1998) 2013–2016.
[11] C.Y. Zhang, H. Ma, S.M. Nie, Y. Ding, L. Jin, D.Y. Chen, Analyst 125 (2000) 1029–1031.
[12] W.H. Liu, M. Howarth, A.B. Greytak, Y. Zheng, D.G. Nocera, A.Y. Ting, M.G. Bawendi, J. Am. Chem. Soc. 130 (2008) 1274–1284.
[13] A.C. Vinayaka, M.S. Thakur, Bioconjugate Chem. 22 (2011) 968–975.
[14] H. Mattoussi, J.M. Mauro, E.R. Goldman, G.P. Anderson, V.C. Sundar, F.V. Mikulec, M.G. Bawendi, J. Am. Chem. Soc. 122 (2000) 12142–12150.
[15] E.R. Goldman, E.D. Balighian, H. Mattoussi, M.K. Kuno, J.M. Mauro, P.T. Tran, G.P. Anderson, J. Am. Chem. Soc. 124 (2002) 6378–6382.
[16] J. Li, K. Zhao, X. Hong, H. Yuan, L. Ma, J.H. Li, Y.B. Bai, T.J. Li, Colloids Surf. B 40 (2005) 179–182.
[17] S.G. Ge, C.C. Zhang, Y.N. Zhu, J.H. Yu, S.S. Zhang, Analyst 135 (2010) 111–115.
[18] Q. Wang, Y.C. Kuo, Y.W. Wang, G. Shin, C. Ruengruglikit, Q.R. Huang, J. Phys. Chem. B 110 (2006) 16860–16866.
[19] Y.C. Kuo, Q. Wang, C. Ruengruglikit, H.L. Yu, Q.R. Huang, J. Phys. Chem. C 112 (2008) 4818–4824.
[20] J.H. Wang, H.Q. Wang, Y.Q. Li, H.L. Zhang, X.Q. Li, X.F. Hua, Y.C. Cao, Z.L. Huang, Y.D. Zhao, Talanta 74 (2008) 724–729.
[21] J.H. Wang, H.Q. Wang, H.L. Zhang, X.Q. Li, X.F. Hua, Z.L. Huang, Y.D. Zhao, Colloids Surf. A 305 (2007) 48–53.
[22] Y.S. Xia, C.Q. Zhu, Talanta 75 (2008) 215–221.
[23] J.B.F. Lloyd, Nature 231 (1971) 64–67.
[24] L. Wang, A.N. Liang, H.Q. Chen, Y. Liu, B.B. Qian, J. Fu, Anal. Chim. Acta 616 (2008) 170–176.
[25] T. Vo-Dinh, Anal. Chem. 50 (1978) 396–401.
[26] L. Li, H.F. Qian, J.C. Ren, Chem. Commun. 4 (2005) 528–530.
[27] Y.Q. Wang, Y.Y. Zhang, F. Zhang, W.Y. Li, J. Mater. Chem. 21 (2011) 6556–6562.
[28] J.P Xie, Y.G Zheng, J.Y. Ying, J. Am. Chem. Soc. 131 (2009) 888–889.
[29] W.W. Yu, L.H. Qu, W.Z. Guo, X.G. Peng, Chem. Mater. 15 (2003) 2854–2860.
[30] Q.G. Liao, Y.F. Li, C.Z. Huang, Talanta 71 (2007) 567–572.
[31] A.N. Liang, L. Wang, H.Q. Chen, B.B. Qian, B. Ling, J. Fu, Talanta 81 (2010) 438–443.
[32] F.P. Yang, Q. Ma, W. Yu, X.G. Su, Talanta 84 (2011) 411–415.
[33] J.L. Duan, X.C. Jiang, S.Q. Ni, M. Yang, J.H. Zhan, Talanta 85 (2011) 1738–1743.
[34] Q. Ma, E.N. Ha, F.P. Yang, X.G. Su, Anal. Chim. Acta 701 (2011) 60–65.